Density of states of a semi-infinite rare-earth metal with magnetic structure: A simple model

Bernardo Laks and G. G. Cabrera
Instituto de Fisica "Gleb Wataghin", Universidade Estadual de Campinas, 13100-Campinas-S.P. Brasil
(Received 10 April 1979)

Using a simple tight-binding model and the transfer matrix approach, we have calculated the spectral density of states (SDOS) of a rare-earth metal in the presence of a surface for different magnetic arrangements (such as ferromagnetic, antiferromagnetic, and conical orderings). The local density of states (LDOS) has also been calculated for some examples, integrating the SDOS over the Brillouin zone. The main effect observed deals with the absence of Van Hove's singularities in the surface LDOS, a fact that appears to be an intrinsic property of the surface. Finally the relaxation of the overlap parameters at the surface is discussed and some numerical examples are shown.

I. INTRODUCTION

Most of the electronic and magnetic properties of the rare-earth metals can be described by a very simple picture: the $4f$ electrons, which determine the magnetic properties, are highly localized while the three outer electrons form a typical conduction band (with $5d$-$6s$ hybridization) in a crystal lattice of trivalent positive ions.

The $4f$ levels are atomiclike in character and no overlap between their atomic wave functions corresponding to neighboring sites is expected. However strong interactions between localized and conduction electrons are present, yielding effective forces between the localized magnetic moments (associated with the $4f$ electrons) in the form of an indirect exchange. The net result is a long-range oscillatory interaction, the Ruderman-Kittel-Kasuya-Yosida (RKKY) interaction,[1] which is responsible for the exotic and diverse spin configurations present in rare-earth metals.[2]

The appearance of different and sometimes complicated magnetic structures will introduce changes in the periodicity of the lattice potential in relation to the paramagnetic crystal lattice. If the new period is commensurate with the former one, the unit cell will be, in general, several times larger, and the corresponding Brillouin zone will be consequently reduced, giving origin to the so-called "new superzone boundaries." When the period of the magnetic structure is not commensurate with that of the paramagnetic crystal lattice we get a system with two kinds of long-range order but no translational symmetry. The situation is similar to the one encountered in antiferromagnetic Cr, where the magnetic ordering is attributed to a spin-density wave.[3]

The magnetic ordering of the localized moments will necessarily affect the band structure associated with the conduction electrons. In the general case, as stated above, the exchange field will have a different symmetry from that of the crystal lattice and alterations in the Fermi surface are expected.[4]

Most of the exotic magnetic arrangements exhibited by rare-earths metals can be described as having an axis of symmetry, which in most cases corresponds to the axis perpendicular to the basal plane in the hcp structure. The order, within each layer perpendicular to the axis, is ferromagnetic and the magnetic moment varies from one layer to the other in direction as well as in magnitude. Simple structures like the ferromagnetic and antiferromagnetic ones are special examples of the general case. In Fig. 1 we give an account of the possible structures considered in this paper.

For this model the original translational symmetry due to the lattice is retained within each layer (which is ferromagnetically ordered), and is only broken along the perpendicular axis which might have no symmetry at all. In the general case, no new broken symmetry appears by introducing a surface, that is a final layer which terminates the crystal.

Since, far from the surface, the localized moments vary in a regular (although nonperiodic) form from one layer to the other, we can study the spectral density of states (SDOS) of conduction electrons by using the transfer matrix approach.[5] The method has been recently applied by a number of authors in order to investigate electronic surface states.[6] It has the great advantage that the method is exact once the Hamiltonian is known and in addition it provides the SDOS directly for the different layers in the crystal. The appearance of surface states can then be straightforwardly tested. Here, our interest is to calculate the SDOS of conduction electrons in a rare-earth metal, and to investigate simultaneously the effects of the surface as well as possible correlations between the different spin arrangements and the SDOS structure.

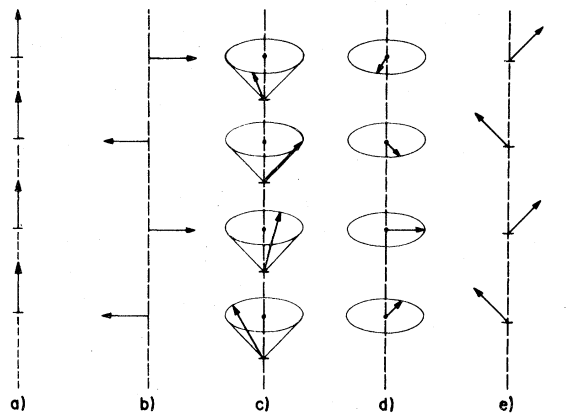

FIG. 1. Some of the different magnetic arrangements presented by the rare-earth metals. The axis shown here is perpendicular to the basal plane and to the surface. The cases depicted here are (a) the ferromagnetic structure; (b) the antiferromagnetic case; (c) a situation of conical ferromagnetism, the angle θ of the cone being fixed and the longitude angle ϕ varying regularly in $\Delta\phi$ from one site to the next along the axis; (d) a helical antiferromagnetic structure, which can be considered a special case of the former one with $\theta=\frac{1}{2}\pi$; and (e) a particular situation of the conical case with $\theta=\frac{1}{4}\pi$ and $\Delta\phi=\pi$.

In Sec. II we write our Hamiltonian using a simple tight-binding model. The exchange between conduction electrons and the localized moments is assumed to be a contact interaction.

In order to use the transfer matrix formalism, it appears more convenient to change spin-site representation, taking as the new quantal axis the local direction of magnetization at each lattice site. Allowing overlapping between nearest-neighbor sites only, we can split the Hamiltonian into two terms: the first one considers coupling between sites on the same layer and is diagonal in the new spin representation; the second part couples neighboring layers and thus introduces spin hybridization.

Possible relaxation effects at the surface are taken into account by varying the overlap parameters between the first two layers and also between different sites on the first layer.

Reconstruction of spin ordering near the surface is not considered as it should be in a self-consistent theory. All through the paper we have used the simplifying assumption of a frozen magnetic structure.

In Sec. III we describe the method used to calculate the SDOS. For some cases, the local density of states (LDOS) has also been calculated, integrating over the two-dimensional Brillouin zone. A brief summary of the transfer matrix approach is also given.

The numerical results and final discussions are presented in Sec. IV. Concerning the LDOS, the main feature seems to be the smoothing out of Van Hove's singularities as one approaches the surface from the bulk, a result which has previously been found using a different method of calculation.[7] In contrast, the SDOS is rich in structures that vary according to the different magnetic arrangements.

No new striking effects are found in the case of an incommensurate spin structure. This is probably due to the fact that rational numbers form a "dense set," i.e., any irrational number can be "very well" approximated by a rational fraction.

When considering surface relaxation we have not found states localized at the surface, even for large variations (more than 20%) of the overlap parameters near the surface. The antiferromagnetic state has been extensively studied since spin hybridization yields the formation of a gap in the SDOS. The search for δ-function singularities split off from the continuous spectrum has been made with negative results.

II. MODEL HAMILTONIAN

Our Hamiltonian is written as a simple tight-binding one in the Wannier representation $|n,\vec{R}_n,\nu\rangle$, where n is the index of the plane, being $n=0$ for the surface; $\vec{R}_n$ is a two-dimensional lattice vector on plane n; and ν is the index of spin which is quantized along the z axis, in a direction perpendicular to the surface.

If $\vec{M}_n$ is the local magnetization on plane n (which is ferromagnetically ordered), the one-site contribution is given by

$$H_{1s}=\sum_{\substack{n\vec{R}_n\\ \nu\nu'}}(\epsilon_0\delta_{\nu\nu'}-J\vec{M}_n\cdot\vec{\sigma}_{\nu\nu'})|n\vec{R}_n\nu\rangle\langle n\vec{R}_n\nu'| \quad , \tag{1}$$

where $\vec{\sigma}$ is the Pauli-spin matrix for conduction electrons.

Allowing hopping between nearest-neighbors sites we add two other contributions: (a) hopping between sites on the same plane

$$H_{2s}=\sum_{\substack{n\vec{R}_n\nu\\ \vec{\Delta}}}t_1(\vec{R}_n,\vec{R}_n+\vec{\Delta})\times|n,\vec{R}_n,\nu\rangle\langle n,\vec{R}_n+\vec{\Delta},\nu| \quad , \tag{2}$$

where $\vec{\Delta}$ runs over the nearest neighbors on the same plane, and (b) hopping between neighboring sites on different planes

$$H'_{2s}=\sum_{\substack{\vec{R}_n,\vec{\delta}\\ n,\delta n\\ \nu}}t_2(n,\vec{R}_n;n+\delta n,\vec{R}_n+\vec{\delta})\times|n,\vec{R}_n,\nu\rangle\langle n+\delta n,\vec{R}_n+\vec{\delta},\nu| \quad . \tag{3}$$

For the simple cubic structure $\delta n=\pm1$ and $\vec{\delta}=0$,

so we write for this case, for t_2 as a real number,

$$H'_{2s} = \sum_{\substack{\vec{R}_n \nu \\ n=0,1,2,\ldots,}} t_2(|n,\vec{R}_n,\nu\rangle\langle n+1,\vec{R}_n,\nu| + \text{H.c.}) \quad . \tag{4}$$

In general we will keep $t_2 \neq t_1$, in order to take into account surface relaxation in subsequent calculations.

Since two-dimensional periodicity is retained within each plane, we can transform to the Bloch representation by using two-dimensional reciprocal vectors $\vec{K}$

$$|n\vec{K}\nu\rangle = \frac{1}{\sqrt{N_2}} \sum_{\vec{R}_n} e^{i\vec{K}\cdot\vec{R}_n} |n\vec{R}_n\nu\rangle \quad , \tag{5}$$

where N_2 is the number of sites per plane.

The total Hamiltonian now can be written

$$H = \sum_{\substack{n\vec{K} \\ \nu\nu'}} [\epsilon(\vec{K})\delta_{\nu\nu'} - J\vec{M}_n\cdot\vec{\sigma}_{\nu\nu'}] |n\vec{K}\nu\rangle\langle n\vec{K}\nu'| + \sum_{\substack{\nu\vec{K} \\ n=0,1,2,\ldots,}} t_2(|n\vec{K}\nu\rangle\langle n+1,\vec{K},\nu| + \text{H.c.}) \quad , \tag{6}$$

where

$$\epsilon(\vec{K}) = \epsilon_0 + t_1 S_{\vec{K}} \quad , \tag{7}$$

and $S_{\vec{K}}$ is a two-dimensional structure factor

$$S_{\vec{K}} = \sum_{\vec{\Delta}} e^{i\vec{K}\cdot\vec{\Delta}} \equiv 4\gamma(\vec{K}) \quad . \tag{8}$$

The first term in relation (6), which we call now H_0, is diagonal in $(n,\vec{K})$ but in general couples the spin numbers due to the local magnetization. The second term in relation (6), which we shall call H_1, is diagonal in $(\vec{K},\nu)$ but couples neighboring planes.

The Hamiltonian H_0 can be diagonalized in spin space by taking the axis of quantization along the local direction of magnetization within each plane.

If $|\alpha\rangle$ and $|\beta\rangle$ are the eigenfunctions of σ_z, we define new states $|\pm\rangle$ by

$$|n\vec{K}+\rangle = e^{-i\phi_n/2}\cos\tfrac{1}{2}\theta_n|n\vec{K}\alpha\rangle + e^{i\phi_n/2}\sin\tfrac{1}{2}\theta_n|n\vec{K}\beta\rangle \quad , \tag{9}$$

$$|nK-\rangle = -e^{-i\phi_n/2}\sin\tfrac{1}{2}\theta_n|n\vec{K}\alpha\rangle + e^{i\phi_n/2}\cos\tfrac{1}{2}\theta_n|n\vec{K}\beta\rangle \quad .$$

In relation (9), $(\theta_n\phi_n)$ are the polar angles of the magnetization for the nth layer.

It may be easily shown that the transformation given by formula (9) diagonalizes H_0, which in the new spin representation takes the form

$$H_0 = \sum_{\substack{n,\vec{K} \\ \mu=\pm}} [\epsilon(\vec{K}) - \mu JM_0] |n\vec{K}\mu\rangle\langle n\vec{K}\mu| \quad . \tag{10}$$

The H_1 Hamiltonian, which describes the coupling between neighboring planes, turns out to be spin hybridized in the new representation. However the coupling constant does not depend on the plane index n for the cases considered in this paper, i.e., when the polar angle θ is constant for all layers $(\theta=\theta_0)$ and ϕ varies regularly from plane to plane (see Fig. 1). If we write $\phi_0=0$ at the surface and $\phi_n = n\Delta\phi$ $(n=0,1,2,3\ldots)$, the H_1 Hamiltonian can be written

$$H_1 = \sum_{\substack{\vec{K} \\ n=0,1,2,\ldots \\ \mu,\mu'=\pm}} t_2[|n\vec{K}\mu\rangle Q_{\mu\mu'}(\theta_0,\Delta\phi) \times \langle n+1,\vec{K}\mu'| + \text{H.c.}] \quad , \tag{11}$$

where $Q(\theta_0,\Delta\phi)$ is a complex (2×2) rotation matrix, which in the new spin representation has the following form:

$$Q(\theta_0,\Delta\phi) = \begin{pmatrix} e^{-i\Delta\phi/2}\cos^2\frac{1}{2}\theta_0 + e^{i\Delta\phi/2}\sin^2\frac{1}{2}\theta_0 & i\sin\theta_0\sin\frac{1}{2}\Delta\phi \\ i\sin\theta_0\sin\frac{1}{2}\Delta\phi & e^{i\Delta\phi/2}\cos^2\frac{1}{2}\theta_0 + e^{-i\Delta\phi/2}\sin^2\frac{1}{2}\theta_0 \end{pmatrix} \quad . \tag{12}$$

We have to point out here that the fact of $Q(\theta_0,\Delta\phi)$ being independent of the layer index yields a set of equations of motion for the resolvent which has a regular pattern. When this is the case we can use the transfer matrix formalism to solve the infinite system of coupled equations.[6] We discuss this point in Sec. III along with the method to calculate the SDOS.

III. METHOD OF CALCULATION

Defining the one-electron resolvent (Green's function) by

$$G(z) = (z-H)^{-1} \quad , \tag{13}$$

where H is the total Hamiltonian, and z is a complex variable, the partial spectral density of states for the subband of spin μ corresponding to the nth layer is obtained as

$$\rho_\mu(n|\vec{K},\omega) \equiv -\frac{1}{\pi}\,\text{Im}\,\langle n\vec{K}\mu|G(\omega+i0^+)|n\vec{K}\mu\rangle \quad . \tag{14}$$

This density of states is properly normalized to unity

$$\int_{-\infty}^{\infty} d\omega\,\rho_\mu(n|\vec{K},\omega) = 1 \quad . \tag{15}$$

The SDOS is obtained by summing over the spin states (in general by summing over the different

types of orbitals)

$$\rho(n\,|\,\vec{K}\omega)=\sum_{\mu=\pm}\rho_\mu(n\,|\,\vec{K}\omega)\ , \tag{16}$$

and is normalized to the number of orbitals per atom considered (in our case 2)

$$\int_{-\infty}^{\infty}d\omega\,\rho(n\,|\,\vec{K}\omega)=2\ . \tag{17}$$

The LDOS, is obtained in turn from the SDOS by summing over the $\vec{K}$ vectors of the two-dimensional Brillouin zone

$$\rho(n\,|\,\omega)\equiv\frac{1}{N_2}\sum_{\vec{K}\in BZ}\rho(n\,|\,\vec{K}\omega)\ , \tag{18}$$

and the normalization is the same as relation (17).

The following notation will prove to be economical:

$$[\underline{G}_{nm}(\vec{K},z)]_{\nu\mu}\equiv\langle n\vec{K}\nu|G(z)|m\vec{K}\mu\rangle\ ; \tag{19}$$

in this sense $\underline{G}_{nm}(\vec{K},z)$ is a (2×2) matrix in spin space.

The equations of motion are obtained through the use of Dyson's equation

$$zG(z)=1+HG(z)\ , \tag{20}$$

yielding an infinite set of coupled equations, which in matrix notation has the following form:

$$(z\underline{1}-\underline{H}_0)\cdot\underline{G}_{0n}=\delta_{n0}\underline{1}+t_2\underline{Q}\cdot\underline{G}_{1n}\ , \tag{21}$$

for all $n=0,1,2,\ldots$;

$$(z\underline{1}-\underline{H}_0)\cdot\underline{G}_{mn}=t_2\underline{Q}^\dagger\cdot\underline{G}_{m-1,n}+t_2\underline{Q}\cdot\underline{G}_{m+1,n}\ , \tag{22}$$

for $0<m<n$;

$$(z\underline{1}-\underline{H}_0)\cdot\underline{G}_{nn}=\underline{1}+t_2\underline{Q}^\dagger\cdot\underline{G}_{n-1,n}+t_2\underline{Q}\cdot\underline{G}_{n+1,n}\ , \tag{23}$$

for $n>0$; and

$$(z\underline{1}-\underline{H}_0)\cdot\underline{G}_{mn}=t_2\underline{Q}^\dagger\cdot\underline{G}_{m-1,n}+t_2\underline{Q}\cdot\underline{G}_{m+1,n}\ , \tag{24}$$

for all $m>n$.

Since the matrices $\underline{Q}$, $\underline{Q}^\dagger$, and $\underline{H}_0$ *do not* depend on the layer index, all the equations (24) have the same pattern. We can define then a transfer matrix[6] by

$$\underline{T}\cdot\underline{G}_{mn}\equiv\underline{G}_{m+1,n}\ , \tag{25}$$

for $m\geq n$. Inserting this definition into equations (24) we get the following matrix equation for $\underline{T}$ (independent of n):

$$t_2\underline{Q}\cdot\underline{T}^2-(z\underline{1}-\underline{H}_0)\cdot\underline{T}+t_2\underline{Q}^\dagger=0\ . \tag{26}$$

In general the latter equation has to be solved numerically: the physical solution is chosen so as to yield a positive density of states, satisfying the boundary condition

$$\lim_{z\to\infty}\underline{T}(z)=0\ . \tag{27}$$

Once the proper solution of $\underline{T}$ is obtained we can compute the SDOS for all layers. As examples we quote the following formulas:

$$\begin{aligned}\underline{G}_{00}(z)&=(z\underline{1}-\underline{H}_0-t_2\underline{Q}\cdot\underline{T})^{-1}\ ,\\ \underline{G}_{11}(z)&=[\underline{G}_{00}^{-1}-t_2^2\underline{Q}^\dagger\cdot(z\underline{1}-\underline{H}_0)^{-1}\cdot\underline{Q}]^{-1}\ ,\\ \underline{G}_{22}(z)&=\{\underline{G}_{00}^{-1}-t_2^2\underline{Q}^\dagger\\ &\quad\cdot[(z\underline{1}-\underline{H}_0)-t_2^2\underline{Q}^\dagger\cdot(z\underline{1}-\underline{H}_0)^{-1}\cdot\underline{Q}]^{-1}\cdot\underline{Q}\}^{-1}\ ,\\ &\ \ \vdots\end{aligned} \tag{28}$$

For getting the bulk density of states $\lim_{n\to\infty}\underline{G}_{nn}(z)$ the procedure is slightly different. In this limit $(n\to\infty)$ the set of equations (22) can be used to define a second transfer matrix by

$$\underline{\Phi}\cdot\underline{G}_{m,n}\equiv\underline{G}_{m-1,n}\ ,\quad 0<m\leq n\ . \tag{29}$$

Inserting this definition into equations (22) we get the following second degree matrix equation for $\underline{\Phi}$:

$$t_2\underline{Q}^\dagger\cdot\underline{\Phi}^2-(z\underline{1}-\underline{H}_0)\cdot\underline{\Phi}+t_2\underline{Q}=0\ , \tag{30}$$

subject to the same boundary condition as $\underline{T}$. Note that $\underline{\Phi}$ and $\underline{T}$ are not the inverse of each other, since they are defined in different subspaces.

Equation (23) now yields

$$\lim_{n\to\infty}\underline{G}_{nn}(z)=[(z\underline{1}-\underline{H}_0)-t_2\underline{Q}^\dagger\cdot\underline{\Phi}-t_2\underline{Q}\cdot\underline{T}]^{-1}\ . \tag{31}$$

The ferromagnetic case is an illustrative example which can be solved analytically in closed form. In this simple case, $\theta_0=0$ and $\Delta\phi$ is arbitrary, and all the matrices involved result in diagonal form:

$$\begin{aligned}\underline{Q}&=\begin{pmatrix}e^{-i\Delta\phi/2}&0\\0&e^{i\Delta\phi/2}\end{pmatrix}\ ,\\ \underline{H}_0&=\begin{pmatrix}\epsilon_+&0\\0&\epsilon_-\end{pmatrix}\ ,\end{aligned} \tag{32}$$

where

$$\epsilon_\pm=\epsilon(\vec{K})\mp JM_0\ . \tag{33}$$

The transfer matrices are also diagonal and direct calculation yields

$$\underline{T}=\begin{pmatrix}\dfrac{e^{i\Delta\phi/2}}{2t_2}\{(z-\epsilon_+)-[(z-\epsilon_+)^2-4t_2^2]^{1/2}\}&0\\0&\dfrac{e^{-i\Delta\phi/2}}{2t_2}\{(z-\epsilon_-)-[(z-\epsilon_-)^2-4t_2^2]^{1/2}\}\end{pmatrix}\ ,$$

and

$$\underline{\Phi}=\begin{pmatrix} \frac{e^{-i\Delta\phi/2}}{2t_2}\{(z-\epsilon_+)-[(z-\epsilon_+)^2-4t_2^2]^{1/2}\} & 0 \\ 0 & \frac{e^{i\Delta\phi/2}}{2t_2}\{(z-\epsilon_-)-[(z-\epsilon_-)^2-4t_2^2]^{1/2}\} \end{pmatrix} .$$

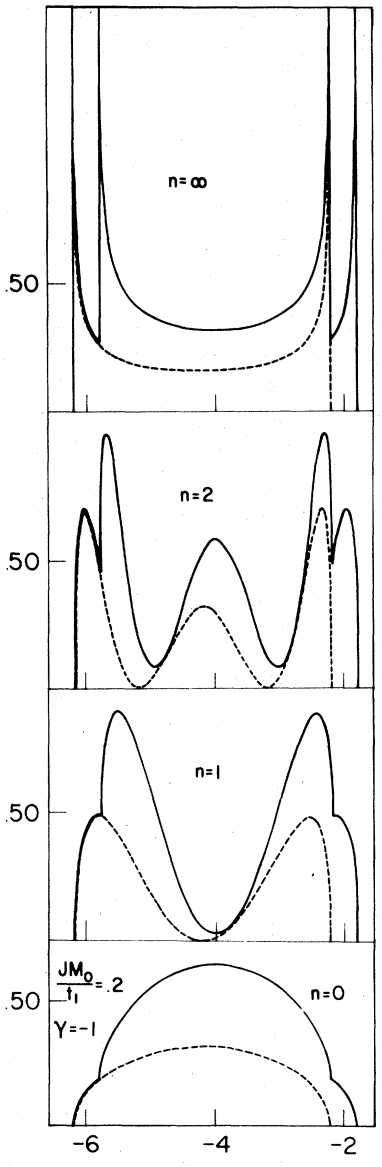

FIG. 2. SDOS for the ferromagnetic case for different layers in the crystal, with $n=0$ the surface and $n=\infty$ the bulk. Here, and in all the next figures, the horizontal axis corresponds to energy in units of t_1. The dashed line illustrates the partial SDOS corresponding to spin +, while the continuous one displays the total SDOS. The exchange splitting has been chosen to be $JM_0/t_1=0.2$ and the SDOS corresponds to a point in the Brillouin zone with $\gamma=-1$. Large oscillations are present in the inner layers, but they are damped as long as we proceed to the interior of the crystal.

Inserting the above results into Eqs. (28) and (31) we get the relevant Green's functions in the form of a continuous fraction

$$(G_{00})_\pm=\{\tfrac{1}{2}(z-\epsilon_\pm)+\tfrac{1}{2}[(z-\epsilon_\pm)^2-4t_2^2]^{1/2}\}^{-1} ,$$

$$(G_{11})_\pm=\left[(G_{00}^{-1})_\pm-\frac{t_2^2}{z-\epsilon_\pm}\right]^{-1} ,$$

$$(G_{22})_\pm=\left[(G_{00}^{-1})_\pm-\frac{t_2^2}{(z-\epsilon_\pm)-t_2^2/(z-\epsilon_\pm)}\right]^{-1} , \quad (34)$$

$$\vdots$$

$$\lim_{n\to\infty}(G_{nn})_\pm=\left[(G_{00}^{-1})_\pm-\cfrac{t_2^2}{(z-\epsilon_\pm)-\cfrac{t_2^2}{(z-\epsilon_\pm)-\cfrac{t_2^2}{\cdots}}}\right]^{-1}$$

$$=[(z-\epsilon_\pm)^2-4t_2^2]^{-1/2} .$$

As it should be from physical considerations, the result is independent of $\Delta\phi$. The corresponding densities of states are shown in Fig. 2 for $t_1=t_2=1$. Note that large oscillations take place when going to the interior of the crystal, increasing the number of states near the band edges and giving rise finally to the four peak structure of the bulk SDOS.

More examples are presented in Sec. IV as well as the final comments.

IV. NUMERICAL RESULTS AND DISCUSSIONS

In the first place we present the results when no surface relaxation is considered. When the parameters at the surface are modified the equations of motion (21) to (24) are slightly different, but the general method of the transfer matrix, described in Sec. III, works perfectly well.

The antiferromagnetic structure is obtained by setting $\theta_0=\frac{1}{2}\pi$ and $\Delta\phi=\pi$. In Fig. 3 we show the corresponding SDOS for various layers (being $n=0$ at the surface and $n=\infty$ in the bulk) for an M point of the two-dimensional Brillouin zone

$$\gamma(\vec{K})=\tfrac{1}{2}[\cos(K_x a)+\cos(K_y a)]=-1 . \quad (35)$$

The strong spin hybridization produces the appear-

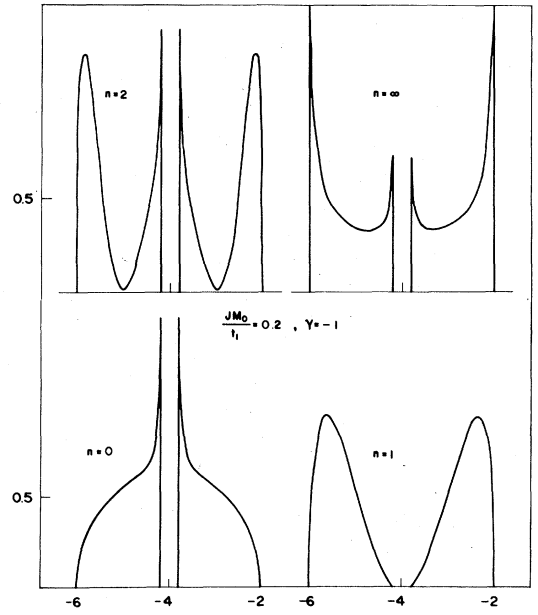

FIG. 3. SDOS for the antiferromagnetic case for a $\gamma=-1$ point in the Brillouin zone. A gap of magnitude $2JM_0/t_1$ appears as a result of spin hybridization. For further comments see the main text.

ance of a gap of magnitude $2JM_0$ in the center of the band for all layers. As in the ferromagnetic case, large oscillations occur when going from the surface to the inner planes. As a common fact we note that for the surface SDOS the states are more concentrated in the neighborhood of the center of the band (and around the gap in the antiferromagnetic case), while for the bulk the availability of states is bigger near the band edges.

In Figs. 4 and 5 we illustrate the surface and bulk SDOS for cases of conical ferromagnetism [like the one shown in part (c) of Fig. 1]. Figure 4 shows a comparison between a case of commensurate spin structure ($\Delta\phi=\frac{1}{5}\pi$) and a noncommensurate case with a value of $\Delta\phi$ close to the former one ($\Delta\phi=0.6$). No striking differences appear; just the formation of little extra kinks in the bulk SDOS for the commensurate case.

The partial contributions corresponding to one-spin subband are also shown in Fig. 5 for the case $\Delta\phi=0.6$. They are slightly asymmetric due to hybridization of the spin states (compare with the partial densities for the ferromagnetic case in Fig. 2).

Figure 6 is the analog of Fig. 4 for two different cases of conical magnetism. We note the appearance of new structures in the form of extra peaks for the bulk density of states and in the form of "ear-shaped" protuberances for the surface SDOS. The origin of the "ears" is again due to spin hybridization, and this fact is illustrated by Fig. 7 showing the partial SDOS for one-spin subband (upper figure) compared to the total SDOS. The partial SDOS for the surface is already highly asymmetric if compared with the ferromagnetic case.

Figure 8 shows the SDOS for interior planes ($n=1,2$) making a comparison between two different cases of conical ferromagnetism. The case in the left ($\theta=\frac{1}{4}\pi$ and $\Delta\phi=\frac{1}{5}\pi$) shows a great resemblance

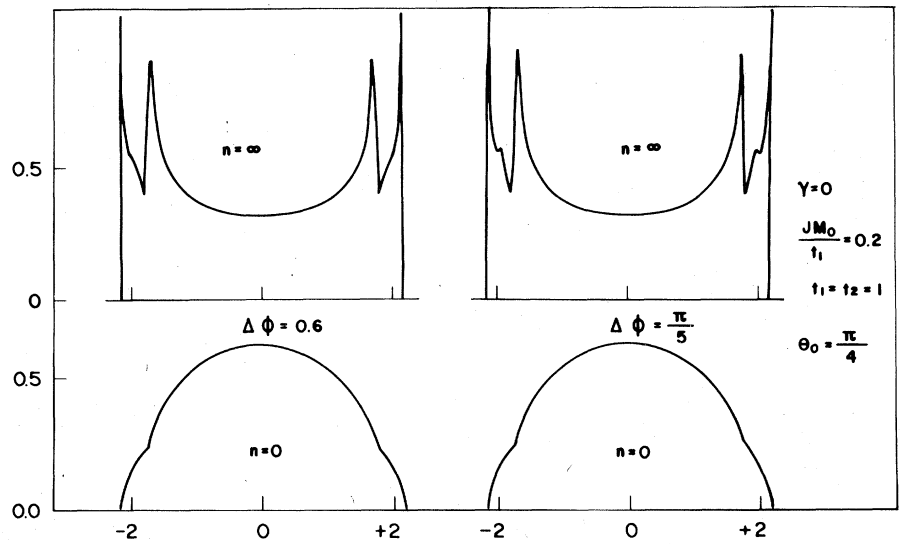

FIG. 4. Surface and bulk SDOS for two different cases of conical ferromagnetism for a $\gamma=0$ point of the Brillouin zone. The case depicted in the left corresponds to a noncommensurate variation of the angle ϕ which will never return to its original value as long as we go to the inner planes. For comparison purposes we display in the same figure a commensurate case where the variation $\Delta\phi$ is close in numerical value to the noncommensurate one.

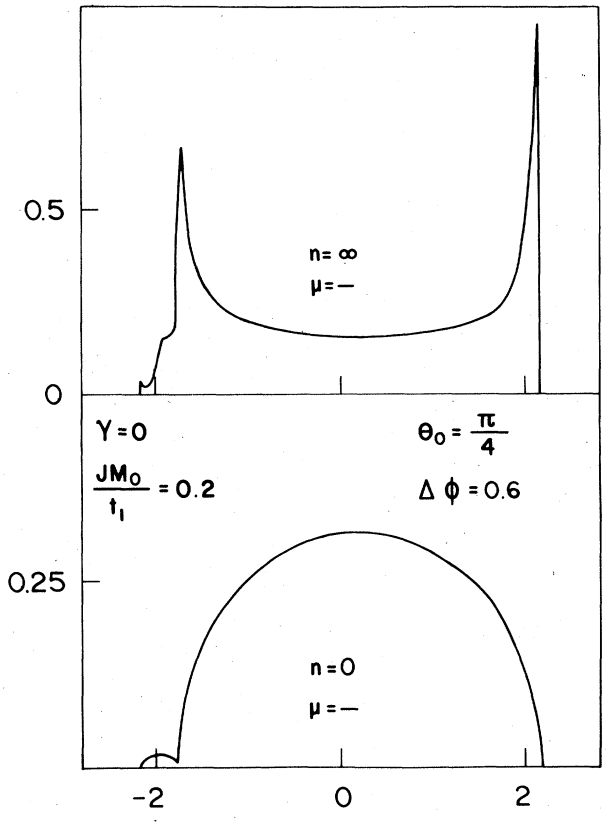

FIG. 5. Partial SDOS for the $\mu=-$ subband corresponding to the noncommensurate case shown in Fig. 4. Spin hybridization has broken the symmetry of the subband.

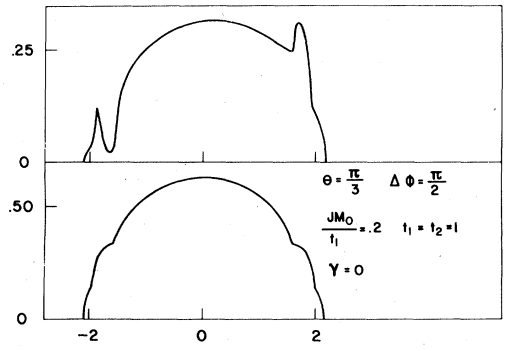

FIG. 7. One-spin partial SDOS compared to the total SDOS for one of the cases shown in the previous figure. The "ears" presented in the total SDOS arise from spin hybridization near the band edges.

with the pure ferromagnetic case.

In Figs. 9–11 we depict the LDOS for ferromagnetism, a case of conical ferromagnetism, and the antiferromagnetic case, respectively. In most instances, 49 points in the two-dimensional Brillouin zone were used to evaluate the LDOS. Near the band edges and singularities the number of points employed was increased until getting convergence. For the ferromagnetic case the analytical expression of the SDOS was known and integrated directly.

In all cases, the Van Hove's singularities have been smoothed out for the surface LDOS. This result has also been reported by Kalkstein and Soven[7] using a different method of calculation, and seems to be an

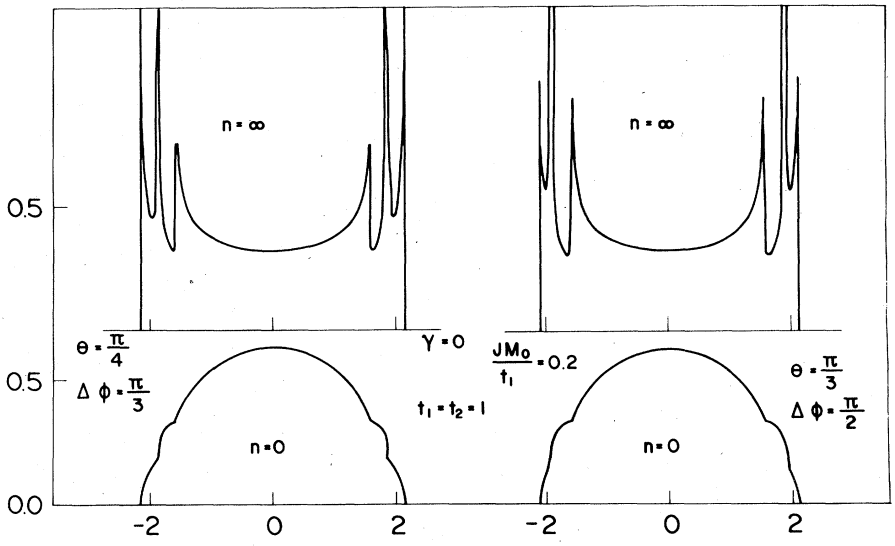

FIG. 6. Surface and bulk SDOS for two different cases of conical ferromagnetism. The point of the Brillouin zone chosen corresponds to $\gamma=0$. The main feature seems to be the appearance of the "ear-shaped" protuberances in the surface SDOS which develop into extra peaks in the bulk case.

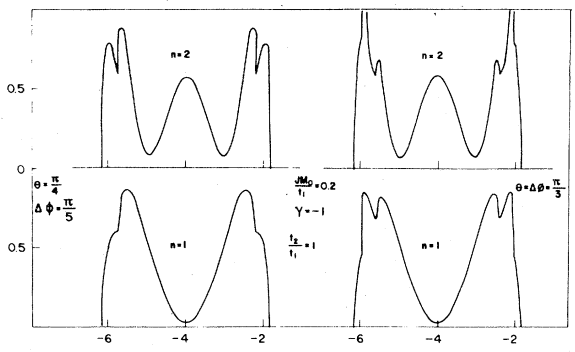

FIG. 8. SDOS for the second and third layers for two examples of conical ferromagnetism and for a point of the Brillouin zone with $\gamma=-1$. The first case is not essentially different from the pure ferromagnetic densities shown in Fig. 2, while the second shows spin hybridization to a larger extent.

intrinsic surface effect. Proceeding to the interior of the crystal the LDOS begins to oscillate and to resemble to the LDOS of an infinite crystal, as it is shown in Figs. 9 and 11. Note that the splitting of Van Hove's singularities near $\omega/t_1=\pm 2$ for the bulk LDOS in Fig. 9 is due to the ferromagnetic exchange $(JM_0/t_1=0.2)$.

In a similar fashion, summing up the antiferromagnetic SDOS over the two-dimensional Brillouin zone yields the formation of a little "pocket" in the center of the band as a reminiscence of the gap which appeared in the SDOS.

Figures 12 to 16 deal with the surface SDOS when the parameters at the surface are varied. In Fig. 12 we have taken a case of conical ferromagnetism and have varied the overlap parameter t_2 at the surface in

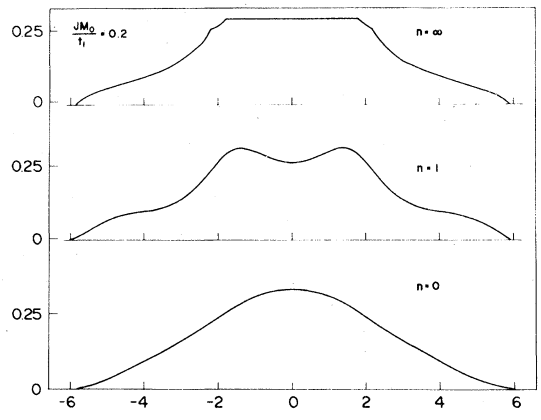

FIG. 9. Local density of states (LDOS) in the ferromagnetic case for the surface, the second layer and the bulk. No Van Hove's singularities are present at the surface with a completely smooth LDOS.

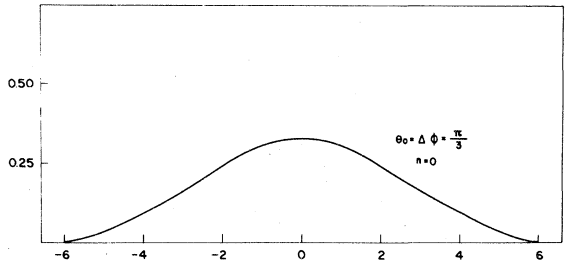

FIG. 10. Surface LDOS for a case of conical ferromagnetism. We found no essential difference in relation to the pure-ferromagnetic case.

both directions: $t_2^s > t_1$ and $t_2^s < t_1$. Remember that t_2^2 is a parameter which describes the overlap between the surface and the next layer. Thus, reducing the value of t_2^s results in a concentration of states near the center of the band, decreasing the mean width. On the contrary, increasing t_2^s results in a surface SDOS which resembles the bulk SDOS with states more concentrated near the band edges. This is precisely what we expect based on physical grounds, since a larger value of t_2^s is equivalent to a surface relaxation, where the first layer gets closer to the second one and consequently the bulk effects are

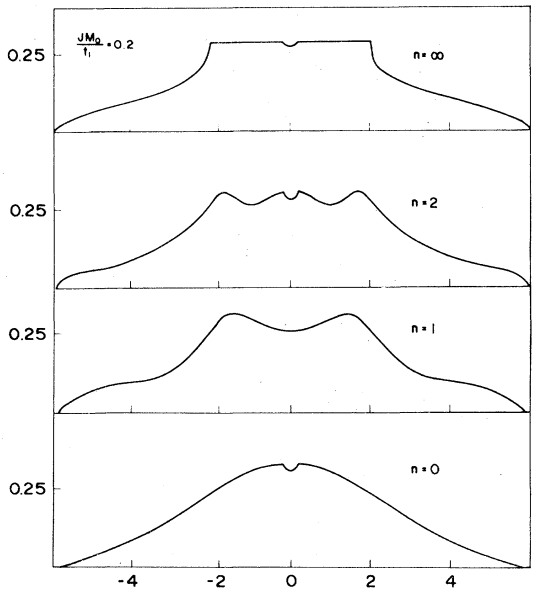

FIG. 11. Antiferromagnetic LDOS for various layers in the crystal. As in the ferromagnetic case no Van Hove's singularities are present at the surface, and oscillations in the LDOS occur while resemblance with the bulk shape increases. The gap present in the SDOS develops, through summation over the entire Brillouin zone, the formation of a little "pocket" in the center of the band.

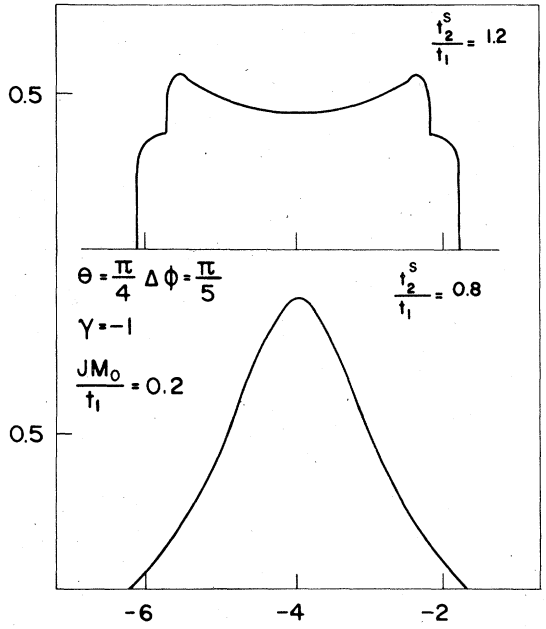

FIG. 12. Surface SDOS when the overlap parameter t_2 is varied at the surface for a case of conical ferromagnetism ($\theta = \frac{1}{4}\pi$, $\Delta\phi = \frac{1}{5}\pi$). In the upper figure the t_2^s parameter (overlap between the surface and the second layer) assumes a value bigger than the bulk case, which corresponds to a situation where the surface relaxes getting closer to the next layer. The net yield is a SDOS for the surface which strongly resembles the bulk case (see Fig. 4). In the lower figure the effect is exactly the contrary; the surface relaxes increasing the distance between the surface and the next layer. Localization of states at the surface should then be bigger.

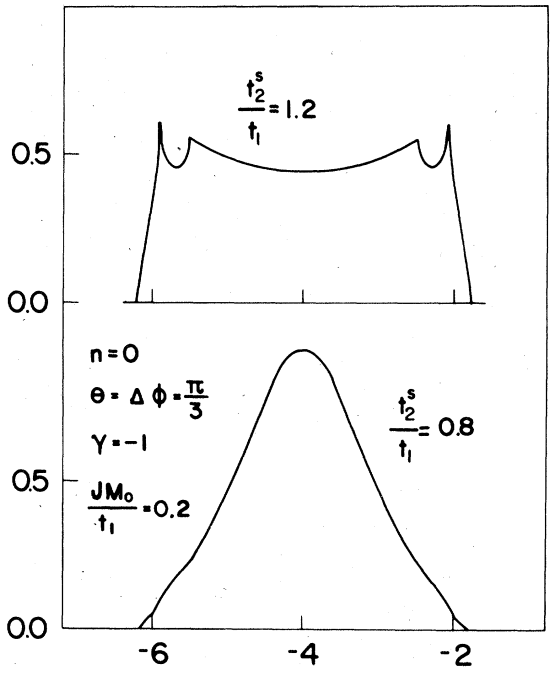

FIG. 13. Same effect depicted by Fig. 12 for a different case of conical ferromagnetism ($\theta = \Delta\phi = \frac{1}{3}\pi$).

then stronger.

Figure 13 shows a similar case for another example of conical ferromagnetism.

In Fig. 14 the parameter t_1, which describes the overlap between neighboring atoms on the surface, is varied, breaking the symmetry of the SDOS. This density of states is reflected around $\omega/t_1 = 4$ for the point $\gamma = -1$.

Figure 15 shows a series of cases where the self-energy ϵ_0^s at the surface is varied along with the exchange splitting JM_0. Varying ϵ_0^s also produces asymmetry in the SDOS in a similar way as in the case when t_1^s is varied.

Finally, in Fig. 16 we depict the antiferromagnetic case when the surface parameters are varied. The roles of varying t_1^s and t_2^s are exactly the same as in the preceding figures. A change in t_1^s produces an asymmetric distribution of the states, while varying t_2^s keeps the symmetry but changes the concentration of states near the gap and band edges. Comparing with Fig. 3 we note that the case $t_2^s < t_1$ presents a larger degree of localization of states around the gap. This situation reflects the fact that t_2 (surface) $< t_2$ (bulk)

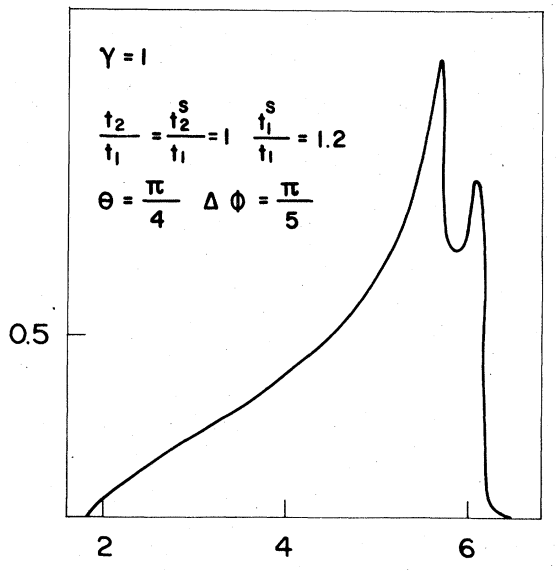

FIG. 14. Here a different case of surface relaxation is shown. The lattice parameter at the surface is shortened, thus enlarging the overlap between neighboring atoms on the layer. The symmetry of the SDOS is lost, but the asymmetric distribution of states is reversed when going to a point with $\gamma = -1$ in the Brillouin zone. Similar results are obtained when the overlap is reduced by the same amount: the same SDOS is reproduced for $t_1^s/t_1 = 0.8$ and $\gamma = -1$.

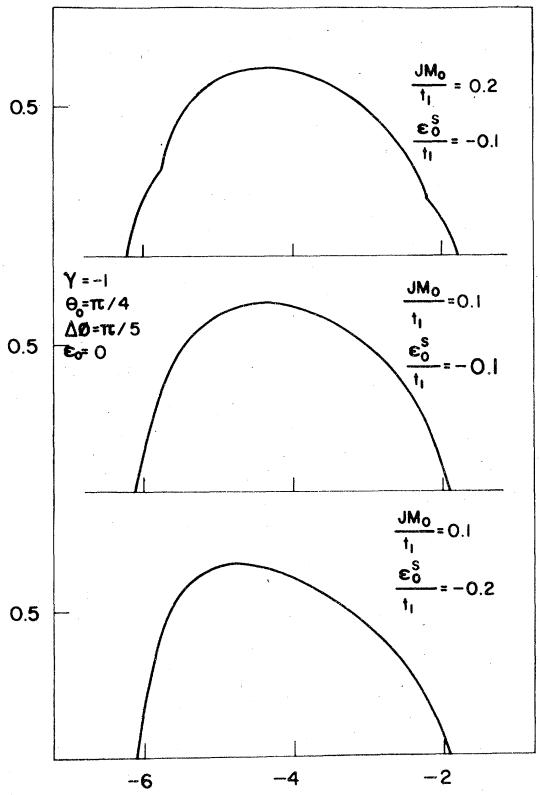

FIG. 15. Varying the parameter ϵ_0 at the surface, here ϵ_0 is the self-energy entering in the dispersion relation $\epsilon(\vec{K}) = \epsilon_0 + 4t_1\gamma(\vec{K})$, produces a similar effect as varying t_1, i.e., a breaking of the symmetry in the SDOS.

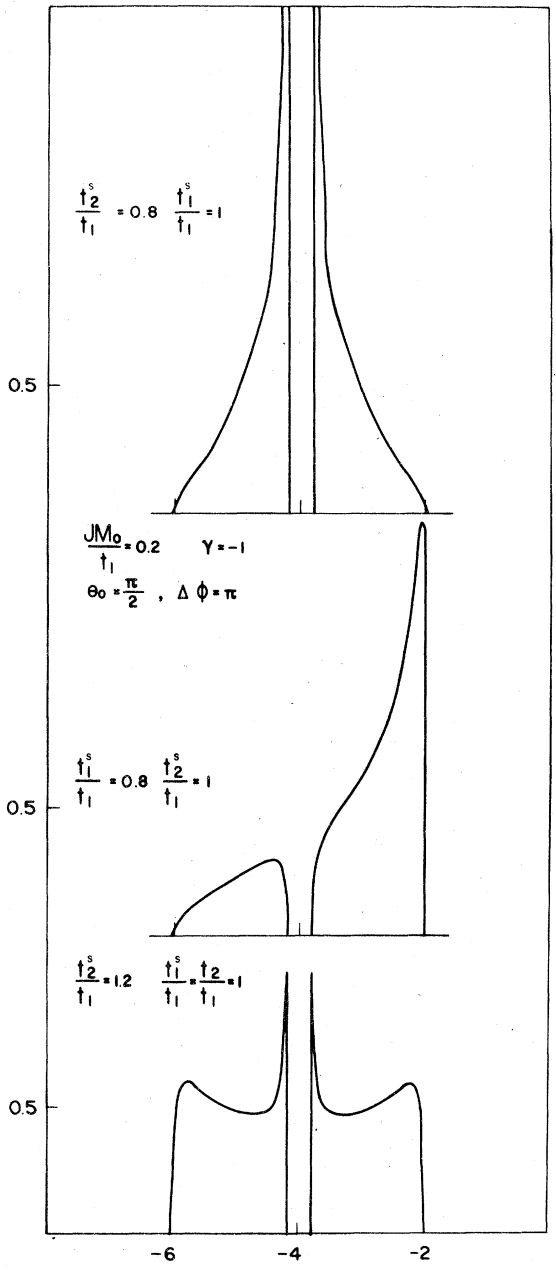

FIG. 16. Surface SDOS for the antiferromagnetic case when the parameters at the surface are varied. For discussions of the different effects see the main text.

is equivalent to the case when the surface relaxes increasing its distance to the next layer. In this case localization of states should be stronger at the surface.

On the other hand, when t_2 (surface) $> t_2$ (bulk) the situation should resemble the bulk case since the surface comes closer to the inner planes.

We have looked for δ-function singularities split-off from the continuous spectrum specially in the gap region. For variations of the surface parameters as those shown here we have not found any intrinisic state localized at the surface in the SDOS.

As a summary we make the following remarks: (i) Due to the experimental techniques existent today, especially photoemission spectroscopy, small regions of the Brillouin zone can be sampled. The SDOS is then the relevant quantity to be calculated and compared to the experiments. (ii) Even when a more realistic model should consider *d-s* hybridization for the conduction band, the general trends here described should be the same. In particular, the energy gap in the antiferromagnetic SDOS, due to strong spin mixing, should also appear. We also feel that the smoothing of Van Hove's singularities in the surface LDOS is also of universal character, being an intrinsic property of the surface. (iii) We have shown here an example where the transfer matrix approach can be used to calculate the SDOS. The method proved to be powerful and of rapid convergence. Apart from providing directly the SDOS (which has more information than the LDOS) for the

surface, we can get without extra work the SDOS for the different layers in the crystal. The intrinsic surface states can then be identified without problem. (iv) The next step in a problem of this kind should be to study spin rearrangements in the vicinity of the surface as a result of possible surface relaxations. A number of works[8] along this line have been carried out for the Heisenberg ferromagnet, yielding magnetic reconstruction with penetration depth of a few layers from the surface.

ACKNOWLEDGMENTS

We are indebted to Professor C. E. T. Gonçalves da Silva who proposed the problem and read the entire manuscript. We also wish to thank Professor J. B. Salzberg for some helpful comments and for reading the final presentation of this material. One of us (G.G.C.) is grateful to CNPq (Conselho Nacional de Desenvolvimento Científico e Tecnológico, Brasil) for partial financial support.

[1]M. A. Ruderman and C. Kittel, Phys. Rev. 96, 99 (1954); T. Kasuya, Prog. Theor. Phys. 16, 45 (1956); 16, 58 (1956), and K. Yosida, Phys. Rev. 106, 893 (1957).

[2]W. C. Koehler, in *Magnetic Properties of Rare Earth Metals,* edited by R. J. Elliott (Plenum, London, 1972), Chap. 3.

[3]C. Herring, in *Magnetism,* edited by G. T. Rado and H. Suhl (Academic, New York, 1966), Vol IV.

[4]R. J. Elliott, in *Magnetism,* edited by G. T. Rado and H. Suhl (Academic, New York, 1965), V. IIA.

[5]B. Laks, Ph.D. thesis (Universidade Estadual de Campinas, 1977) (unpublished).

[6]L. M. Falicov and F. Yndurain, J. Phys. C 8, 1563 (1975); B. Laks and C. E. G. Gonçalves da Silva, Solid State Commun. 25, 401 (1978); 25, 561 (1978); and C. E. T. Gonçalves da Silva and B. Laks, J. Phys. C 10, 851 (1977).

[7]D. Kalkstein and P. Soven, Surf. Sci. 26, 85 (1971).

[8]C. Demangeat and D. L. Mills, Phys. Rev. B 14, 4997 (1976); J. C. S. Levy and Diep-The-Hung, Phys. Rev. B 18, 3593 (1978).